The morphology of Au@MgO nanopeapods

2009 Nanotechnology 20 455603

(http://iopscience.iop.org/0957-4484/20/45/455603)

Nanotechnology **20** (2009) 455603 (6pp) doi:10.1088/0957-4484/20/45/455603

The morphology of Au@MgO nanopeapods

W W Zhou[1], L Sun[1], T Yu[1], J X Zhang[2], H Gong[2] and H J Fan[1,3]

[1] Division of Physics and Applied Physics, School of Physical and Mathematical Sciences, Nanyang Technological University, 21 Nanyang Link, 637371, Singapore
[2] Division of Materials Science and Engineering, National University of Singapore, 117576, Singapore

E-mail: fanhj@ntu.edu.sg

Received 12 August 2009
Published 16 October 2009
Online at stacks.iop.org/Nano/20/455603

Abstract

The structure of metal nanoparticles embedded inside dielectric nanowires/nanotubes, namely nanopeapods, has been of increasing interest due to their unusual photoresponse and optical adsorption properties. This paper presents a type of new inorganic nanopeapod: faceted Au nanoparticles inside MgO nanowires. The Au self-assembles into a nanoparticle chain during the vapor–liquid–solid growth of the MgO nanowires for which gold also serves as the catalyst. Surprisingly such a chain can follow the whole axis of the MgO nanowires even if the latter zigzag, provided that the amount of gold is sufficient. It is shown that such Au@MgO nanopeapods form not only under metalorganic chemical vapor deposition conditions (Lai *et al* 2009 *Appl. Phys. Lett.* **94** 022904), but also under our conventional vapor transport deposition condition. This new nanopeapod material might be a candidate for the study of electronic and/or plasmonic wave transport along nanowires.

(Some figures in this article are in colour only in the electronic version)

Nanowires of dielectric materials such as SiO_2, Al_2O_3, MgO, and complex oxides like perovskite $Pb(ZrTi)O_3$ and $BaTiO_3$ have been one of the focuses of nanoscience research [1–12]. Such nanostructures can be the host for spintronic devices and nanocapacitors, or agents for advanced ceramics to improve dielectric behavior [13–16]. In particular, the nonlinear optical properties of a dielectric material can be tailored by embedding discrete metal nanoparticles in it. A typical known example is Ag in glass [17, 18]. It was recently demonstrated that the surface plasmon resonance of a periodic Au nanostructure sandwiched by a $Pb(ZrTi)O_3$ layer can be both red shifted and blue shifted up to ∼120 nm by the piezoelectricity of the $Pb(ZrTi)O_3$ film [19]. Lee *et al* demonstrated that the third-order susceptibility of a $(Ba, Sr)TiO_3$ film dispersed with gold nanoparticles (∼3.8 nm) is maximized near the surface plasmon resonance of gold [20]. In case of MgO, it has long been reported that the surface plasmon resonance wavelength of ion-implanted Au nanoparticles within MgO can be shifted in the range of 524–560 nm depending on the post-annealing atmosphere [21]. Such a shift has been proposed to stem from the existence of quantum antidots at the surface of Au nanoparticles, and associated electron transfer from Au nanoparticles to the quantum antidots [22, 23]. In these studies, the Au nanoparticles were implanted into a MgO film; it is expected that on a nanoscale, the nonlinear optical properties of MgO nanowires should be also influenced by the existence of Au nanoparticles. Indeed, the surface plasmon of Au nanoellipses has been shown to contribute to the enhanced photosensibility of SiO_2 and Ga_2O_3 nanowires [24, 25]. The self-assembly of metal nanoparticles into MgO nanowires into a type of nanopeapod structure, as we will demonstrate in this paper, might provide a suitable candidate for the above mentioned studies.

Similar nanopeapod structures have been observed in SiO_2 [25–27] and Ga_2O_3 nanowires [24] which were formed *in situ* through self-assembly with a gold catalyst. Recently, large quantities of nanopeapods of $Pt@CoAl_2O_4$ and $Cu@Al_2O_3$ have also been intentionally fabricated by a German group in a process involving Rayleigh instability [28, 29]. While the fabrication of MgO nanowires has been intensively studied by various groups using different methods [4, 30–34, 11, 35, 36], there are few reports on the formation of Au@MgO

[3] Author to whom any correspondence should be addressed.

nanopeapods. During the preparation of this manuscript Lai *et al* mentioned in passing the nanopeapod structure in their growth optimization experiments on MgO nanowires by metal organic chemical vapor deposition [30]. However, no details on the structural properties or growth mechanism were given.

In this paper, we report in more detail the morphology and possible growth mechanism of Au@MgO nanopeapods. We found that such a structure occurs very frequently during the vapor–liquid–solid (VLS) growth of MgO nanowires through a simple vapor transport and deposition process. The gold nanoparticles are faceted rather than elliptical, and can exist throughout all the axes of the nanowires.

Nanowire growth was conducted inside a horizontal quartz tube furnace via a vapor transport and deposition method. The source material, Mg_3N_2 powder (Alfa Aesar, 99.5%), was put inside a small quartz tube (inner diameter 12 mm, length 15 cm) and located at the center of the heating zone. Oxidized silicon substrates or MgO(001) crystal were deposited with ≈3 nm thick gold film by sputtering, and located 2–3 cm downstream inside the small quartz tube. The small tube (with powder and substrate) was inserted into a larger one (25.4 mm diameter). The temperature near the source and the substrate was about 900 and 800 °C, respectively. Mg vapor obtained by thermal decomposition of Mg_3N_2 was transported downstream and reacted with the trace oxygen. The total pressure inside the quartz tube was maintained at either 200 or 10 mbar by Ar gas flow (100 sccm) and pumping. The structure and crystallography of the samples were investigated using field emission scanning electron microscopy (FESEM; JEOL JEM-1400F), transmission electron microscopy (TEM; Philips CM20T), and high-resolution TEM (JEOL JEM-4010).

Previously MgO nanowires have been grown either by vapor transport and deposition, pulse laser deposition (PLD), or metalorganic chemical vapor deposition (MOCVD). In all these experiments, gold is used as a catalyst for the VLS process. For our MgO nanowire growth experiments, the resulting morphology is found to be very sensitive to the level of oxygen partial pressure, which is consistent with the findings in other work [4]. A general result of our experiments is as follows: if MgO(001) epitaxial substrates are used, the nanowires are vertically aligned and unidirectional; in case of Si substrate, however, the nanowires have random alignment and a long length (>10 μm) and generally have a 90° zigzag shape (see figure 1). The zigzag shape can appear at ambient pressures of both 10 and 200 mbar [37]. The reason for this is unknown, but is most likely related to diffusion of the catalyst [35]. Similar zigzag shaped or branched MgO nanowires were also previously reported by Li *et al* [38] and Hao *et al* [4], using a metal Mg source. The reason for the zigzag shape is most likely due to thermodynamic fluctuation of the liquid–solid interface caused by instability of the growth parameters, such as temperature or pressure. Hence, the direction of growth easily changes between the equivalent ⟨100⟩ directions. On the other hand, those MgO nanowires fabricated by PLD have nearly no zigzag shape [24, 31, 34, 36]. This might be due to the fact that in the PLD process the temperature and vapor partial pressure are under better control.

Our MgO nanowires are single crystalline and are also believed to grow via a VLS mechanism, as indicated by the Au tip in figure 2.[4] A major distinction from previous reports is that during our TEM observations it was found that more than 50% of the MgO nanowires, even from different growth batches, have gold embedded in their interiors, forming a peapod structure (see figure 3). The gold was confirmed by energy dispersive x-ray spectroscopy (EDX) line scan across two particles, as shown in figure 2(c). This shows the Au signal only at the particle sites whereas a uniform profile of Mg and O. Such peapods are found to appear more often at 10 mbar than at 200 mbar, which again might be related to the catalyst diffusion that occurs more easily at a lower pressure, according to Yanagida *et al* [35]. Interestingly, even when the nanowire suddenly changes its growth direction, the Au chain also follows the zigzag (see figures 3(a) and (d)). The nanoparticles have a quasi-periodical distribution. For certain nanowires, a transition from a continuous gold line to individual particles is observed near the ends of the MgO nanowire, as indicated by white arrows in figure 4. This phenomenon is similar to the often-observed Au@SiO_2 nanopeapods. However, the observation of such a nanopeapod structure in MgO is very rare. Based on inspection of many other TEM images and the VLS growth mechanism, we expect that the gold locates at the growing fronts rather than the nanowire roots.

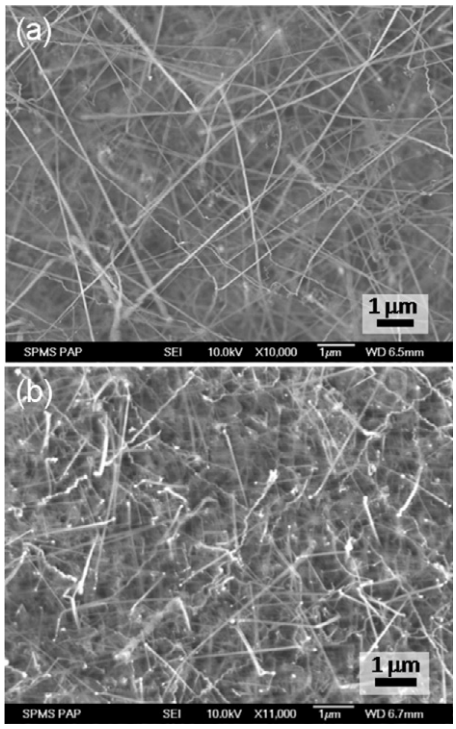

Figure 1. SEM images of MgO nanowires. Note the zigzag morphology, especially in (b).

Another peculiarity of Au@MgO nanopeapods is that the gold particles are single crystalline and faceted, as revealed by the high-resolution TEM images in figure 5. This is in contrast to the elliptical Au nanodots embedded in SiO_2 nanowires. Such faceting is attributed to the single

[4] Most nanowires are broken by sonication during TEM sample preparation, so that Au is not present at all the nanowire ends.

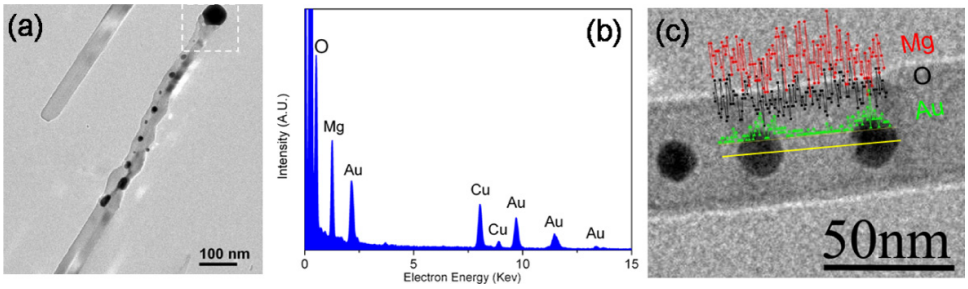

Figure 2. (a) One incomplete Au@MgO nanopeapod showing the Au particles on the nanowire tip as well as in the bulk. (b) EDX spectrum recorded near the tip indicated in (a) showing that the particle is Au and the growth is initiated by the vapor–liquid–solid process. (c) EDX line scan across two particles showing the elements of Au, Mg, and O.

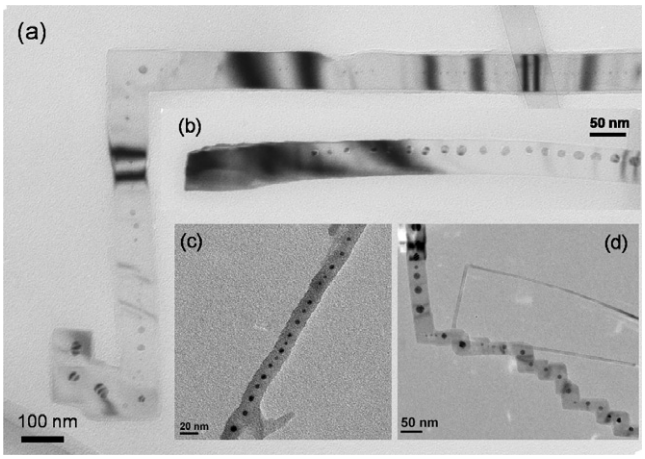

Figure 3. TEM images of several Au@MgO nanopeapods. The MgO nanowires in (a) and (d) are 90° zigzagged due to a switch in growth direction between the equivalent ⟨100⟩ directions.

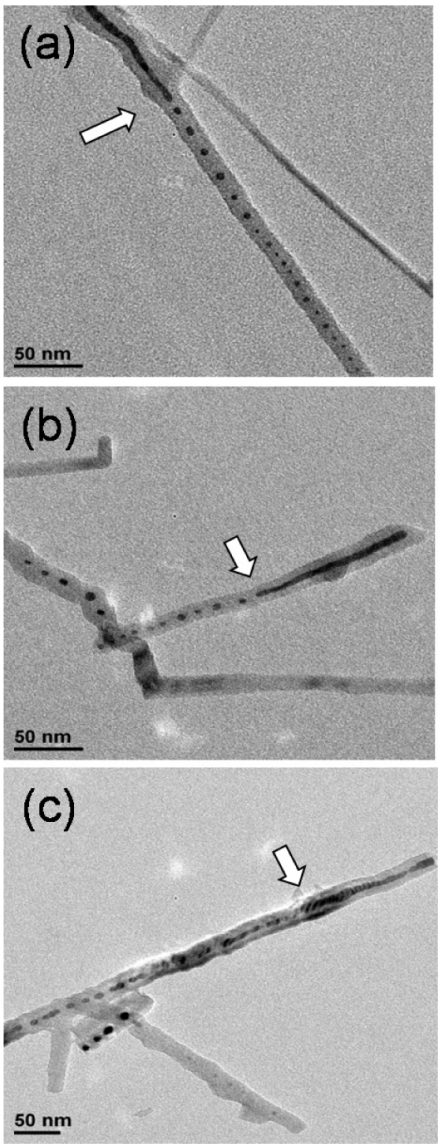

Figure 4. TEM images of some of Au@MgO nanopeapods showing the continuous Au nanowire core close to the growth fronts. The white arrows indicate the transition from Au wire into discrete particles.

crystalline characteristic of the MgO nanowires compared to the amorphous SiO_2. In the crystalline surroundings, the Au particles tend to reduce the total surface energy by forming facets. The Au nanoparticles have the shape of a partially truncated octahedron (as shown by the schematic model). Their overall shapes in figures 5(a)–(d) are a result of projection of different special orientations of the octahedron [39]. Two examples are given in figures 5(e) and (f) to show how they fit respectively to figures 4(c) and (d) by rotation.

The lattice structures of MgO(200) and Au(111) and Au(100) are clearly resolved. Both Au and MgO have a face-center-cubic structure with lattice constants of $a_{\mathrm{MgO}} = 0.421$ nm and $a_{\mathrm{Au}} = 0.408$ nm. Therefore an epitaxial interface is expected in their major planes. This is indeed the case in figure 5, where a relationship of Au(001) ∥ MgO(001) is established, as indicated in figure 5(c). This is consistent with the findings by Wang *et al* [22] in their TEM investigation of implanted Au nanoparticles inside MgO substrates, in which the same epitaxial interface was inferred based on the cubic faceting of the generated vacancy clusters (i.e. antidots).

Table 1 summarizes the so-far reported inorganic nanopeapods formed either through *in situ* self-assembly during VLS growth of nanowires or by heating induced defragmentation of initially continuous gold cylinders within a central channel of nanowires (i.e. Rayleigh instability). Since the MgO nanowires in our experiments are solid, the mechanism must differ from those in cases 4–6. For cases

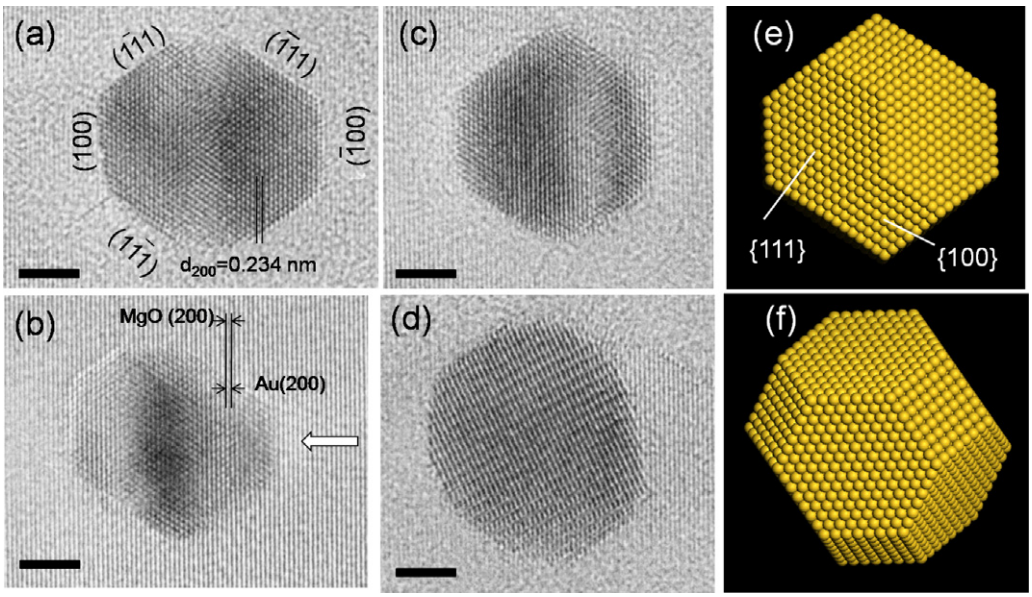

Figure 5. (a)–(d) HRTEM images of the gold nanoparticles embedded inside single crystalline MgO nanowires. Labeled in (a) are facet planes of Au in the Au [011] zone axis. The white arrow in (b) indicates the growth direction of MgO is along [001]. An orientation relationship of Au(001) ‖ MgO(001) can be inferred. Scale bar: 3 nm. A schematic 3D model of a partially truncated octahedral structure is shown in (e)–(f), where (e) corresponds to (c) and (f) to (d).

Table 1. A summary of metal-inside-nanowire peapod nanostructures.

No.	Material	Proposed formation mechanism	Ref
1	$Au@SiO_2$	Oxide induced instability at the nanowire front	[26]
2	$Au@Ga_2O_3$	Phase separation induced by the formation of twin boundaries	[24]
3	$Au_2Si@SiO_2$	Growth instability at the nanowire root	[27]
4	$Au@SiO_2$	Flow of gold into a hollow channel	[25]
5	$Cu@Al_2O_3$	Fragmentation of confined Cu nanowires and Rayleigh instability	[29]
6	$Pt@CoAl_2O_4$	Release of Pt segments into a hollow channel and Rayleigh instability	[28]
7	Au@MgO	Oxide induced instability at the nanowire front	[30] and this work

1–3 two different mechanisms were proposed, as indicated in table 1: the first is a top-down 'flow of gold' process. For case 1, the AuSi atop the nanowires is squeezed into the wire body by the growing SiO_2 sheath; for case 2, non-uniform supersaturation (higher at edges than at the center) takes place during the significant fluctuation in temperature, so that crystallization prevails around the catalyst droplet. In both cases, the instability is induced by the faster growth/oxidation immediately surrounding the edges of the liquid droplets than at the liquid–solid interface. The second mechanism (case 3) is a bottom-up process in which the Au–Si composite nanowires grow from the silicide islands. The pre-formed Au–Si nanowires in the core break into a chain of Au_2Si nanospheres due to growth instability (namely, a periodic change of the melting curvature). A common feature for both mechanisms is that the metal nanochains are formed by pinching off a metal cylinder due to the instability of such cylinders.

In our case of Au@MgO, the gold particles are found at the growth fronts (see figures 1(b) and 2(a)). It is conceived that the mechanism should differ from the second one but may be similar to that for cases 1 and 2. Figure 6 shows schematically our proposed formation process. The possible chemical reactions include

$$Mg_3N_2\ (s) \rightarrow Mg\ (v) + N_2$$

$$Mg\ (v) + Au\ (l) \rightarrow MgAu\ (alloy)$$

$$Mg\ (l) + O_2 \rightarrow MgO\ (s).$$

At the growth temperature of 800 °C, Au can alloy with Mg to form a Au-rich eutectic according to the phase diagram. Upon supersaturation in the liquid alloy the Mg precipitates and is simultaneously oxidized into MgO just near the edge of the liquid–solid interface (oxygen comes from trace air in the chamber). The growth is relatively fast ($\sim$2 μm min^{-1} on Si substrates) so that part of the gold can remain at the core as a continuous cylinder before precipitation at the center of the liquid–solid interface. When the gold nanowire core reaches a certain length it becomes unstable and then transforms into discrete nanoparticles. When the gold is not completely consumed at the growing ends, a section of continuous gold core remains near the ends, as seen in figure 4.

Coming back to the zigzag morphology, as mentioned earlier, the MgO nanowires were grown via VLS with

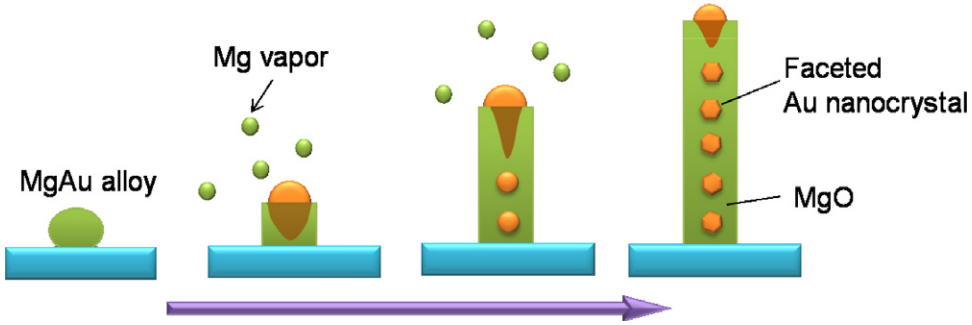

Figure 6. A proposed formation process for Au@MgO nanopeapods.

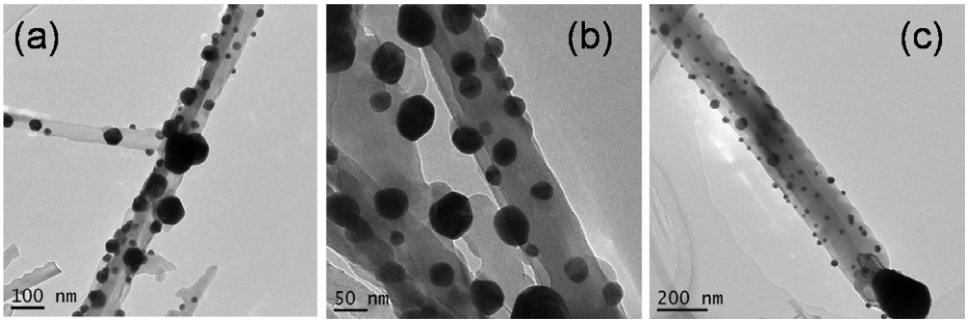

Figure 7. Structures of Au-nanoparticle-attached MgO nanowires after annealing in air ambient at 700 °C for 2 h. One can see the agglomeration of gold nanoparticles but no evident sinking of gold into the MgO either from the edges or from the tip.

the AuMg eutectic droplet as catalyst. The synthesis process, thermal evaporation followed by vapor transport and deposition, is a non-equilibrium one, in that the temperature and Mg vapor partial pressure can fluctuate significantly. Hence instability occurs at the liquid–solid interface, leading to changes in the growth direction. Following this process, Au nanoparticles dislodge from the eutectic tip forming peapods. In addition, we also found such zigzag or branched MgO nanowires without gold embedding, especially for the growth at 200 mbar [37]. This corroborates our proposal that the peapods are formed via a 'top-down' process along the nanowires during the VLS growth, as schematically shown in figure 6.

It has been reported that Fe can diffuse into MgO near 600 °C, for example during the Fe-catalyzed growth of carbon nanotubes on MgO [40], and during the growth of perovskites on Pt/MgO/Fe layers [41]. In order to examine the possibility that gold diffuses from the MgO nanowire surface into the bulk, a control experiment was conducted. Gold nanoparticles of diameter 15 ± 3 nm were attached to the surface of MgO nanowires which were immersed into a colloidal suspension. The sample was then annealed in air at 800 °C for 8 h. TEM observation (see figure 7) shows only surface agglomeration and formation of large Au particles or maybe slight sinking into the nanowire body [42], but no penetration into the bulk of MgO nanowires. In addition, as seen in figure 7(c), a large Au particle atop one nanowire did not flow into the wires. This corroborates that the structures shown in figures 3 and 4 are formed *in situ* during the growth of MgO nanowires, similar to the proposed mechanism for Au@SiO_2 and Au@Ga_2O_3 nanopeapods [24, 26].

In conclusion, we present clear evidence of Au@MgO nanopeapod structures, which appear frequently during the vapor-phase growth of MgO nanowires using Au film as a catalyst. This kind of hybrid structure may have interesting nonlinear optical applications as induced by the surface plasmon resonance of the Au particles, provided that the Au particle size and distance can be tuned by further optimizing growth conditions or employing new growth techniques (e.g. microwave enhanced chemical vapor deposition).

Acknowledgments

We thank Dr R Scholz (MPI-Halle) for performing some of the TEM investigations, and Z Zhang and T Wu (Nanyang Technological University) for the use of their furnace and useful discussions. Start-up funding from NTU for H J Fan is highly appreciated.

References

[1] Alexe M, Hesse D, Schmidt V, Senz S, Fan H J, Zacharias M and Gösele U 2006 Ferroelectric nanotubes fabricated using nanowires as positive templates *Appl. Phys. Lett.* **89** 172907

[2] Fang X S, Ye C H, Zhang L D and Xie T 2005 Twinning-mediated growth of Al_2O_3 nanobelts and their enhanced dielectric responses *Adv. Mater.* **17** 1661–5

[3] Han S, Li C, Liu Z Q, Lei B, Zhang D H, Jin W, Liu X L, Tang T and Zhou C W 2004 Transition metal oxide core–shell nanowires: generic synthesis and transport studies *Nano Lett.* **4** 1241–6

[4] Hao Y F, Meng G W, Zhou Y, Kong M G, Wei Q, Ye M and Zhang L D 2006 Tuning the architecture of MgO nanostructures by chemical vapour transport and condensation *Nanotechnology* **17** 5006–12

[5] Kawasaki S, Fan H J, Catalan G, Morrison F D, Tatsuta T, Tsuji O and Scott J F 2008 Solution-process coating of vertical ZnO nanowires with ferroelectrics *Nanotechnology* **19** 5

[6] Kim G, Martens R L, Thompson G B, Kim B C and Gupta A 2007 Selective area synthesis of magnesium oxide nanowires *J. Appl. Phys.* **102** 104906

[7] Lee W, Scholz R and Gösele U 2008 A continuous process for structurally well-defined Al_2O_3 nanotubes based on pulse anodization of aluminum *Nano Lett.* **8** 2155–60

[8] Liu L F *et al* 2008 Synthesis, characterization, photoluminescence and ferroelectric properties of $PbTiO_3$ nanotube arrays *Mater. Sci. Eng.* B **149** 41

[9] Rorvik P M, Almli A, van Helvoort A T J, Holmestad R, Tybell T, Grande T and Einarsrud M A 2008 $PbTiO_3$ nanorod arrays grown by self-assembly of nanocrystals *Nanotechnology* **19** 225605

[10] Shimpi P, Gao P X, Goberman D G and Ding Y 2009 Low temperature synthesis and characterization of MgO/ZnO composite nanowire arrays *Nanotechnology* **20** 125608

[11] Yanagida T, Marcu A, Matsui H, Nagashima K, Oka K, Yokota K, Taniguchi M and Kawai T 2008 Enhancement of oxide VLS growth by carbon on substrate surface *J. Phys. Chem.* C **112** 18923

[12] Zhang X Y, Zhao X, Lai C W, Wang J, Tang X G and Dai J Y 2004 Synthesis and piezoresponse of highly ordered $Pb(Zr_{0.53}Ti_{0.47})O_3$ nanowire arrays *Appl. Phys. Lett.* **85** 4190–2

[13] Catalan G and Scott J F 2009 Physics and applications of bismuth ferrite *Adv. Mater.* **21** 2463–85

[14] Cohen R 2009 Nanocapacitors: undead layers breathe new life *Nat. Mater.* **8** 366–8

[15] Kong L B, Zhang T S, Ma J and Boey F 2008 Progress in synthesis of ferroelectric ceramic materials via high-energy mechanochemical technique *Prog. Mater. Sci.* **53** 207–322

[16] Scott J F 2007 Applications of modern ferroelectrics *Science* **315** 954–9

[17] Dubiel M, Yang X, Schneider Y R, Hofmeister H and Schicke K D 2004 Structure and properties of nanoparticle glass composites *7th European-Society-of-Glass Conf. on Glass Science and Technology* (Athens: Soc. Glass Technology) pp 148–52

[18] Takeda Y and Kishimoto N 2002 Nonlinear optical properties of metal nanoparticle composites for optical applications *13th Int. Conf. on Ion Beam Modification of Materials* (Kobe: Elsevier Science Bv) pp 620–3

[19] Chen H L, Hsieh K C, Lin C H and Chen S H 2008 Using direct nanoimprinting of ferroelectric films to prepare devices exhibiting bi-directionally tunable surface plasmon resonances *Nanotechnology* **19** 435304

[20] Lee K S, Lee T S, Kim I H, Cheong B and Kim W M 2004 Optical properties of Au nanoparticle dispersed (Ba, Sr)TiO_3 thin films *16th Int. Symp. on Integrated Ferroelectrics/5th Korean Workshop on High Dielectric Devices and Materials (Gyeongju)* pp 295–302

[21] Ueda A *et al* 1998 Interaction of Fn-centers with gold nanocrystals produced by gold ion implantation in MgO single crystals *Nucl. Instrum. Methods Phys. Res.* B **141** 261–7

[22] Wang C M, Shutthanandan V, Thevuthasan S and Duscher G 2005 Direct imaging of quantum antidots in MgO dispersed with Au nanoclusters *Appl. Phys. Lett.* **87** 153104

[23] Xu J, Moxom J, Overbury S H, White C W, Mills A P and Suzuki R 2002 Quantum antidot formation and correlation to optical shift of gold nanoparticles embedded in MgO *Phys. Rev. Lett.* **88** 175502

[24] Hsieh C-H, Chou L-J, Lin G-R, Bando Y and Golberg D 2008 Nanophotonic switch: gold-in-Ga_2O_3 peapod nanowires *Nano Lett.* **8** 3081–5

[25] Hu M-S, Chen H-L, Shen C-H, Hong L-S, Huang B-R, Chen K-H and Chen L-C 2006 Photosensitive gold-nanoparticle-embedded dielectric nanowires *Nat. Mater.* **5** 102–6

[26] Kolb F M, Berger A, Hofmeister H, Pippel E, Gösele U and Zacharias M 2006 Periodic chains of gold nanoparticles and the role of oxygen during the growth of silicon nanowires *Appl. Phys. Lett.* **89** 173111

[27] Wu J S, Dhara S, Wu C T, Chen K H, Chen Y F and Chen L C 2002 Growth and optical properties of self-organized Au_2Si nanospheres pea-podded in a silicon oxide nanowire *Adv. Mater.* **14** 1847–50

[28] Liu L F, Lee W, Scholz R, Pippel E and Gösele U 2008 Tailor-made inorganic nanopeapods: structural design of linear noble metal nanoparticle chains *Angew. Chem. Int. Edn* **47** 7004–8

[29] Qin Y, Liu L, Yang R, Gösele U and Knez M 2008 General assembly method for linear metal nanoparticle chains embedded in nanotubes *Nano Lett.* **8** 3221–5

[30] Lai Y F, Chaudouet P, Charlot F, Matko I and Dubourdieu C 2009 Magnesium oxide nanowires synthesized by pulsed liquid-injection metal organic chemical vapor deposition *Appl. Phys. Lett.* **94** 022904

[31] Nagashima K, Yanagida T, Tanaka H and Kawai T 2007 Epitaxial growth of MgO nanowires by pulsed laser deposition *J. Appl. Phys.* **101** 124304

[32] Nagashima K, Yanagida T, Tanaka H, Seki S, Saeki A, Tagawa S and Kawai T 2008 Effect of the heterointerface on transport properties of *in situ* formed MgO/titanate heterostructured nanowires *J. Am. Chem. Soc.* **130** 5378–82

[33] Takeshi Y, Kazuki N, Hidekazu T and Tomoji K 2008 Mechanism of critical catalyst size effect on MgO nanowire growth by pulsed laser deposition *J. Appl. Phys.* **104** 016101

[34] Yan Y G, Zhou L X, Zhang J, Zeng H B, Zhang Y and Zhang L D 2008 Synthesis and growth discussion of one-dimensional MgO nanostructures: nanowires, nanobelts, and nanotubes in VLS mechanism *J. Phys. Chem.* C **112** 10412–7

[35] Yanagida T, Nagashima K, Tanaka H and Kawai T 2007 Mechanism of catalyst diffusion on magnesium oxide nanowire growth *Appl. Phys. Lett.* **91** 061502

[36] Yanagida T, Nagashima K, Tanaka H and Kawai T 2008 Mechanism of critical catalyst size effect on MgO nanowire growth by pulsed laser deposition *J. Appl. Phys.* **104** 016101

[37] Fan H J, Knez M, Scholz R, Nielsch K, Pippel E, Hesse D, Gösele U and Zacharias M 2006 Single-crystalline $MgAl_2O_4$ spinel nanotubes using a reactive and removable MgO nanowire template *Nanotechnology* **17** 5157–62

[38] Li Y, Bando Y and Sato T 2002 Preparation of network-like MgO nanobelts on Si substrate *Chem. Phys. Lett.* **359** 141–5

[39] Barnard A S, Lin X M and Curtiss L A 2005 Equilibrium morphology of face-centered cubic gold nanoparticles >3 nm and the shape changes induced by temperature *J. Phys. Chem.* B **109** 24465–72

[40] Zhang Q, Zhao M Q, Huang J Q, Qian W Z and Wei F 2008 Selective synthesis of single/double/multi-walled carbon nanotubes on MgO-supported Fe catalyst *14th Int. Congress on Catalysis* (Dalian: Science China Press) pp 1138–44

[41] Matsumoto T, Tamai K, Murashima Y, Komaki K and Nakagawa S 2009 Effect of Fe diffusion in MgO/Fe seedlayers to attain (100) oriented Pt underlayer for perovskite films with *c*-axis orientation *ICMAT: Int. Conf. on Materials for Advanced Technologies (Singapore)*

[42] Ajayan P M and Marks L D 1989 Evidence for sinking of small particles into substrates and implications for heterogeneous catalysis *Nature* **338** 139–41